Vol. 485: 105–121, 2013
doi: 10.3354/meps10309

MARINE ECOLOGY PROGRESS SERIES
Mar Ecol Prog Ser

Published June 27

Turbulent mixing limits mussel feeding: direct estimates of feeding rate and vertical diffusivity

Camille Saurel[1,3,*], Jens Kjerulf Petersen[2], Philip J. Wiles[1], Michel J. Kaiser[1]

[1]School of Ocean Sciences, College of Natural Sciences, Bangor University, Menai Bridge, Anglesey LL59 5AB, UK
[2]The Danish Shellfish Centre, 7900 Nykøbing Mors, Denmark

[3]*Present address:* IMAR — Institute of Marine Research, Centre for Ocean and Environment, IMAR-DCEA, Fac. Ciencias e Tecnologia, 2829-516 Monte da Caparica, Portugal

ABSTRACT: Field measurements of physical and biological parameters, together with the estimation of mass transport and estimation of clearance rates (for feeding rate) using a biodeposition method (defecation) were combined to improve the understanding of the limiting factors that affect the feeding rate of blue mussels in an intertidal commercial re-laid benthic mussel bed. The study used an *in situ* feeding rate method to describe one of the mechanisms that underpins mussel bed self-patterning. The feeding rate of mussels measured using the *in situ* method (defecation) closely matched the rate of the measured turbulent transport of chl *a*. This relationship suggested that the supply rate of food limited the growth of mussels in this system. Vertical food depletion ([chl *a*] <1 µg l^{-1}; height <6 cm) was measured above the mussel bed, and horizontal food depletion (at 5 cm above the bed) was measured in the water column at both mussel patches as well as at adjacent bare patches and in between. Mussel size mirrored the measured food gradient such that larger mussels occurred at the edge compared with the middle of the patches of mussels. In this system, the high mussel feeding rate (2.9 l $ind.^{-1}$ h^{-1}), despite food depletion near the mussel bed, is due to the interaction of 3 hydrodynamic processes: vertical turbulent mixing, advection and re-suspension. These processes are themselves altered through a positive feedback mechanism associated with the mussel bed morphology. We found that the highest feeding rates are achieved when mussel beds are interspersed with patches of bare mud; thus stocking strategies that promote the formation of self-patterning should be encouraged.

KEY WORDS: *Mytilus* · Aquaculture · Stocking · Mass transport · Clearance rate · Biodeposition · *In situ* · Benthic boundary layer

INTRODUCTION

Mussels (family Mytilidae) are a dominant component of benthic biomass in the coastal zone (Seed & Suchanek 1992), and are considered to be facilitators, as they are habitat-forming organisms and provide shelter for other species (Bruno et al. 2003). Mussels have a substantial grazing impact on phytoplankton biomass due to their high water processing potential (Cloern 1982, Fréchette & Bourget 1985a,b, Petersen 2004). In addition, they provide an important source of food for human consumption with global landings of 1.9 million tonnes in 2010 (FAO 2012).

The depletion by mussels of suspended particulate matter and phytoplankton can influence downstream food availability for other mussels and suspension-feeders both within and beyond mussel beds (Tweddle et al. 2005, Simpson et al. 2007). Food depletion in the benthic boundary layer (BBL) has been detected both in the laboratory and *in situ* (Fréchette & Bourget 1985a,b, Monismith et al. 1990, Fréchette et al. 1993, Butman et al. 1994, O'Riordan et al. 1995,

*Email: camillesaurel@hotmail.com

Dolmer 2000) as well as within mussel cultivation areas (e.g. Petersen et al. 2008). Food depletion in mussel beds will lead to a reduction in mussel suspension feeding (Newell et al. 2001, Riisgård 1991, Saurel et al. 2007) and eventually to reduced mussel growth. The latter varies according to the position of the mussel within the dense mussel bed (Fréchette & Bourget 1985a, Svane & Ompi 1993).

Dense mussel beds can filter large volumes of water, up to 170 m^3 m^{-2} d^{-1} (Jørgensen et al. 1990, Prins et al. 1996). Consequently, food supply is a product of hydrodynamic transport processes that impact upon food concentration that in turn is a critical factor that determines mussel production and hence the extent and density of a mussel bed (Larsen & Riisgård 1997). Tidal advection and vertical turbulent flux are important factors that affect the supply of food to the BBL. Mussel beds impact upon these processes as they modify water flow at different scales: (1) at a micro scale (mm to cm) by increasing bed roughness via both biomixing created by the jet of water from the exhalant siphons (Monismith et al. 1990, Lassen et al. 2006, van Duren et al. 2006) and via the mussel shell shape and dense and extensive mussel aggregations (Butman et al. 1994), and (2) at a macro scale (tens of meters), via the topographic variation of the mussel bed, e.g. alternation between mussel patches and bare patches of sediment (Butman et al. 1994).

In many coastal areas, hydrodynamics and food availability change at many spatial and temporal scales that are influenced by factors such as tides, seasons, weather and geomorphology. These variations make it difficult to link mussel production to local hydrodynamics and food availability. Some studies have focused on bivalve feeding in the BBL (Fréchette et al. 1993), but it is difficult to measure fluxes of material over bivalve beds. One of the main issues in the past decades is the level of intrusion and detail of accuracy of the instruments used to make such measurements. For instance, empirical measurements and modelling undertaken in a flume (Butman et al. 1994) were developed to understand the physical and biological processes that occur at small spatial and temporal scales to test and validate the model of Fréchette et al. (1989). Nevertheless, as Butman et al. (1994) noted, natural conditions differ considerably from controlled laboratory conditions. More recent *in situ* studies have focused on the effect of hydrodynamics on the supply of food to the benthos (Jones et al. 2009, Monismith et al. 2010) through the comparison of feeding rates to hydrodynamics using non-invasive *in situ* methodologies (e.g. acoustic Doppler current profiler, acoustic Doppler velocimeters, *in situ* fluorometer, phytoplankton sampling devices.). However, such studies often lack the appropriate biophysical measurements in a control site without filter-feeding bivalves to confirm that the food depletion close to the bed is due to bivalve filtration per se and not from other processes (e.g. hydrodynamic).

In this study we used the concept of 'ask the animals — ask the water' (Petersen 2004) and simultaneously measured (1) water column parameters such as hydrodynamic forcing and seston composition above a mussel bed and nearby bare sand using non-intrusive instrumentation, and (2) mussel parameters such as clearance rate and feeding behaviour using *in situ* defecation methodology (Kotta & Møhlenberg 2002, Kotta et al. 2005, Saurel 2008) and continuous video recording of mussel feeding behaviour (Saurel et al. 2007). We tested 2 hypotheses: (1) mussel filtration is the factor responsible for food depletion in the BBL above a mussel bed, and (2) mussel bed self-organisation (Gascoigne et al. 2005, van de Koppel et al. 2008, de Jager et al. 2011) is directly related to the interaction between feeding rates and the hydrodynamic processes that spatially affect food supply (i.e. phytoplankton) (Butman et al. 1994). Ultimately, we aimed to generate the empirical evidence to support a conceptual model of food supply dynamics in relation to mussel bed patchiness. Furthermore, we aimed to calculate how the interaction between hydrodynamics, food supply and animal feeding controls the production capacity of mussels in commercially laid intertidal mussel beds.

MATERIALS AND METHODS

The study site was located in the Menai Strait, North Wales, United Kingdom where the annual mussel production of ~10 000 t represents half the UK annual production and come from a growing area of ~700 ha. Experiments were undertaken during July 2006 (Fig. 1) when the immersion time of the mussel beds due to the tide was ~6 h. The mussels are cultivated on a mud substratum. The seed mussels (<15 mm length) are generally collected from subtidal ephemeral mussel beds and then re-laid intertidally or subtidally (Beadman et al. 2004, Saurel et al. 2004, 2007). In this system, food concentration is low for most of the year (~1 µg chl *a* l^{-1}) but can vary from 0.5 up to 5 µg l^{-1} during the spring/summer season.

We measured the chlorophyll *a* concentration [chl *a*] in the water column at different heights above the seabed using a repeated-measures design across

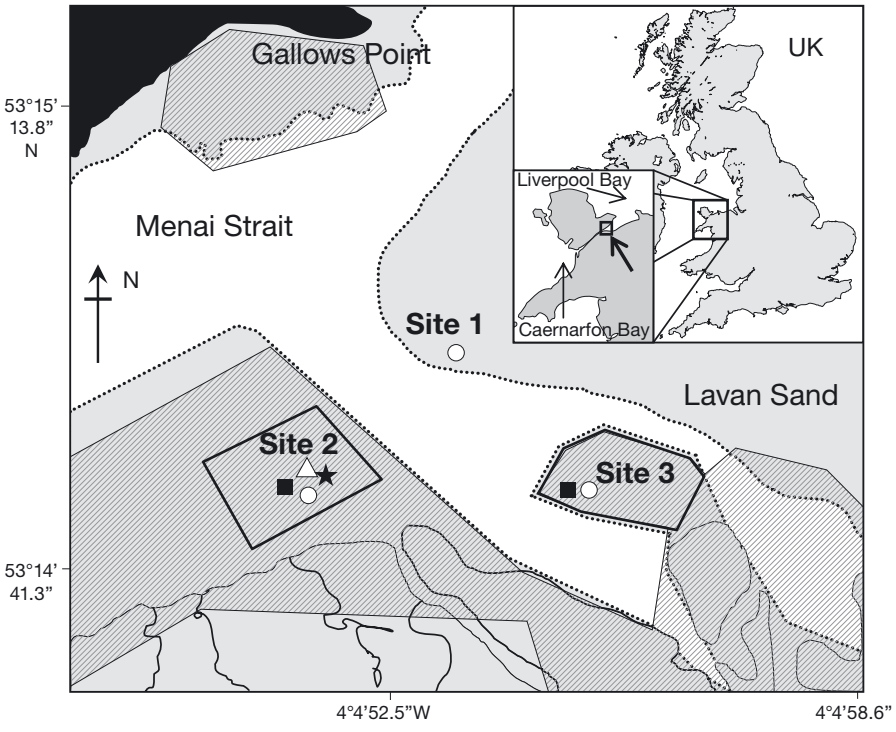

Fig. 1. Experimental sites and the position of the instruments during July 2006. Site 1: bare substrate (sand); Site 2: a young mussel bed; Site 3: an old mussel bed. ○: siphon mimics, ■: acoustic doppler current profiler (ADCP); ★: camera; △: fluorometer; dotted line: mean low water; grey area: intertidal area; striped area: mussel bed

a single tidal cycle at each of the following 3 contrasting sites. The null hypothesis tested was that there was no difference in the vertical gradient of chl *a* concentrations between 2 different mussel coverage conditions (mussels present or mussels absent) at each time of sampling. Site 1 was a control treatment (no mussels) and was characterised by a sandy seabed, Site 2 was a relatively new mussel bed (with mussels and bare substratum patches) and Site 3 an older mussel bed (with mussels and bare substratum patches) (Figs. 1 & 2). The distance between the sites is given in Table 1. Mussels from Sites 2 and 3 were composed of a single cohort. Three sets of experiments designed to study the interactions between hydrodynamics, mussels and seston were set up at different spatial scales (Fig. 2).

Hydrodynamics

The spatial difference in the water velocity that occurred over the intertidal commercial mussel bed (over the 3 sites) was mapped with a roving RDI 1.2 MHz Workhorse acoustic doppler current profiler (ADCP) during a survey on 30 June 2006. The ADCP was attached to the side of a 5 m long boat and bottom tracking was used to account for the motion of the boat and hence calculate the true water current velocity. A GPS unit was used to determine the position of velocity measurements. Initial analyses from the roving ADCP data showed that spatial variation occurred in current direction and speed over the entire intertidal bed but that similar types of current regimes occurred at the 3 sites chosen for the experiment.

Time series of vertical velocity profiles were measured using a bottom mounted RDI 1.2 MHz ADCP. The ADCP was initially buried into the sediment at Site 2 (July 14, 15) and then at Site 3 (July 16–18; Fig. 1). The ADCP sampled current velocities at 1.25 Hz with a vertical bin size of 0.25 m. The variance method (Stacey et al. 1999) was used to estimate Reynolds stresses from the ADCP data. An averaging period of 8 min was used. Because the measured Reynolds stresses were close to the noise threshold (Williams & Simpson 2004), the velocity shear and Reynolds stresses were split into segments of 24.84 h and tidally phase-averaged to create one 24.84 h time series. The 24.84 h averaging period was used as the tide had both a diurnal and semidiurnal component, i.e. the amplitude of the later tide was smaller than the earlier tide. The data were rotated into 'along stream' and 'across stream' components that varied throughout the tide (see Fig. 3). The vertical diffusivity (diffusion coefficient

Table 1. Site descriptors. NA: not applicable

Site	% mussel cover	Position	Area covered by mussels (m^2)	Mussel age	Time from re-laying	Distance between sites (km)
1 Sand	NA	53°14′54″N, 4°05′46″ W	NA	NA	NA	1 to 2 = 0.588
2 Mussel bed	63.3	53°14′43″ N, 4°06′12″ W	36 714	~1 yr	~1 mo	2 to 3 = 0.668
3 Mussel bed	40.3	53°14′45″ N, 4°05′36″ W	18 538	>1 yr	~1 yr	3 to 1 = 0.333

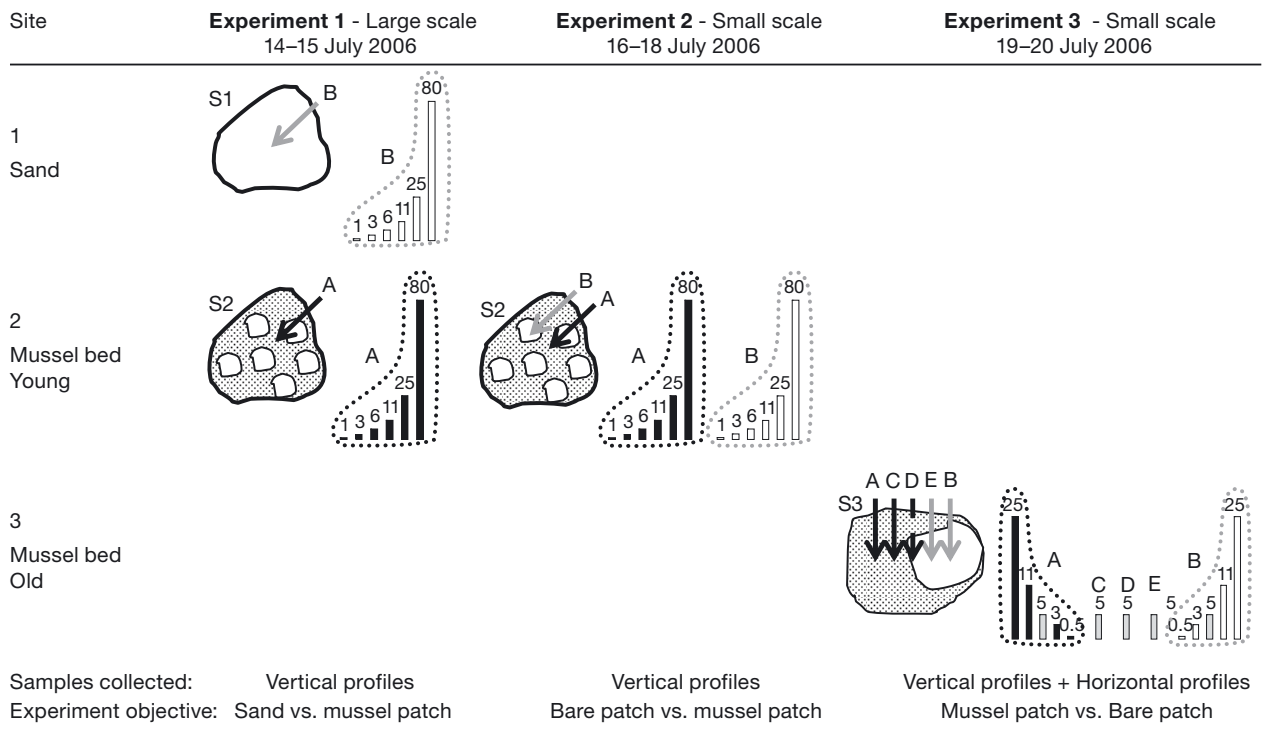

Fig. 2. Experimental set up at the 3 sites (S1–3). White areas: sandy or bare sediment patches; dotted areas: mussel patches. Siphon mimics (SM; A–E) are represented by vertical bars, indicating the height (cm) of sampling above the bed (white: above bare/sandy patch; black: above mussel patch; grey: horizontal profile). Grey arrows: SM sampling above bare/sandy patch; black arrows: above mussel patch; broken arrow: above the edge of the mussel patch

K_z) was estimated for the bottom 4 bins (at heights 0.49, 0.74, 0.99 and 1.24 m above the bed) of the ADCP data using the measured Reynolds stresses and velocities (Rippeth et al. 2002). In this near-bed region, both the phase-averaged Reynolds stresses and velocity shear were above the ADCP noise threshold. K_z was estimated from the ADCP data according to:

$$K_z \sim N_z = \tau/(\mathrm{d}u/\mathrm{d}z) \quad (1)$$

where N_z is the eddy viscosity, τ is the Reynolds' stress and $\mathrm{d}u/\mathrm{d}z$ is the variation of velocity with height (Rippeth et al. 2002). A straight line was then fitted to the K_z values (forced through 0 at the bed) in order to obtain a value for K_z at 0.05 m above the bed. This straight line fit near the bed is an approximation on the parabolic curve as given in Rippeth et al. (2002). The eddy diffusivity K_z is assumed to be equal to the eddy viscosity (Fréchette et al. 1989).

A completely independent estimate of K_z was made from the animal (mussels) and seston concentration [chl *a*] according to:

$$K_z(\mathrm{d}[\text{chl } a]/\mathrm{d}z) = \text{feeding} \quad (2)$$

where $\mathrm{d}[\text{chl } a]/\mathrm{d}z$ is the variation of chl *a* concentration with height.

The time for vertical mixing (t_v) was estimated using Lewis (1997) (this equation refers to the diffusion of a spreading patch of dye):

$$t_v = \sigma^2{}_z/2K_z = (0.8h)^2/2K_z = 0.32h^2/K_z \quad (3)$$

Vertical mixing is assumed to be complete when the standard deviation (σ) of a distribution of tracer (e.g. phytoplankton) equals 0.8 h, where h is the total water depth (Lewis 1997).

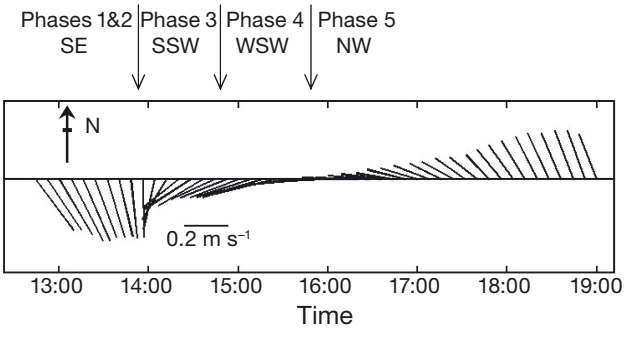

Fig. 3. Example of depth-averaged current velocity and direction (m s^{-1}) time series from the ADCP represented by vectors over Site 2 on July 17 with arbitrary determined phases of the tide in function of current direction (see Table 7). The origin of the vector is on the horizontal line. Over the whole sampling period, similar data were measured

Seston concentration: vertical and horizontal [chl *a*] profiles

Three sets of experiments were carried out on the intertidal area (Figs. 1 & 2). Water samples were collected by pumping water at a flow speed of 90 ml min^{-1} through mussel siphon mimics (SM) consisting of plastic tubing with an open diameter of 2 mm. Each siphon (tube length <20 m) was buried in the sediment for a length of ~5 m to avoid interference with current flow and re-suspension of material. The free end of the SM tubes were attached to a buoy to enable collection of samples via a peristaltic pump mounted onboard an anchored boat.

For Expts 1 and 2 (Fig. 2), 2 sets of 6 tubes were positioned at 0.5, 3, 6, 11, 25 and 80 cm above the surface of the seabed and 3 replicates samples of water from the 2 sets were collected simultaneously from 2 small boats for ~5 min every 30 min for 3 to 4 h. For Expt 3 (Fig. 2), 2 sets of siphons were positioned at 1, 3, 5, 11 and 25 cm above the surface of the seabed, 1 set located in the middle of the mussel patch and the other in the adjacent bare patch; 3 additional siphons at 5 cm height above the seabed were positioned in between the 2 sets of siphons: in the edge zone of the mussel patch, at the interface between the mussel and sand patch and in the edge zone of the sand patch. Each of these 5 siphons at 5 cm height was approximately 50 cm from its nearest neighbour(s). Using this arrangement of the SMs, a horizontal transect with 5 SMs at height of 5 cm and separated by ~50 cm intervals was established between the 2 sets of vertical profiles.

A SCUFA (Self-Contained Underwater Fluorescence Apparatus) submersible fluorometer (Turner Designs) was positioned in the middle of the mussel bed at Site 2 to record the pattern of fluorescence as a measure of [chl *a*] above the mussel bed.

Mussels

Feeding behaviour

A waterproof digital camera (NIKON 4500) together with a timer (Digisnap) was deployed on the seabed next to the ADCP on Site 2 for the whole period of the experiment (Fig. 1). Mussel feeding behaviour of approximately ~30 ind. was determined from still images taken every 10 min and measured with an image analysis program, analySIS©. Variation in feeding behaviour was expressed as the mean percentage valve gape aperture, exhibited by the mussels in the field of view (Saurel et al. 2007).

Mussel population parameters

Three replicate mussel samples were taken using a 15 cm diameter cylindrical core at the middle and edge of patches next to the SM. A subsample of 30 mussels was taken and shell length (*L*, mm) for each mussel measured. The dry weight (DW, g) of mussel flesh was obtained by drying for at least 24 h at 90°C. The density of the mussel was then calculated (Table 2). Mussel size (shell length) was used as a proxy for growth, as mussel seeds from the same cohort were randomly distributed in the bed 1 mo prior to the sampling at Site 2 or the year before at Site 3. Mortality was not taken into account in this study.

The percentage of mussel cover at each of the different sites (Table 1) was calculated from aerial photographs taken at low tide using a helium inflatable balloon fitted with a camera and connected by a rope to the photographer located within the mussel bed a couple of days prior to the experiment. A known length of tape provided a means of scaling the images from the photographic survey. Fourteen pictures from Sites 2 and 3 were analysed with ImageJ v1.37 freeware: images were RGB colour split, and mussel percentage cover were calculated automatically.

Clearance rate

Mussel *in situ* clearance rate was estimated using the defecation method (Saurel 2008). Mussels from the mussel-covered intertidal area in Site 2 were collected from the boat using a rake after the sampling occurred using the SMs. They were then placed individually in 1 l buckets filled with seawater and allowed to defecate for 1 h. Faecal pellets were col-

Table 2. Results of morphometric measurements at the different sites and positions within *Mytilus edulis* mussel beds (±1 SD). Shell length (*L*), n = 30; Condition Index (CI) = (DW/*L*) × 1000, n = 20 ind.

Parameter	Density (ind. m^{-2})	*L* (mm)	CI
Site 2			
Edge	3640 ± 605	34.5 ± 4.0	15.1 ± 2.4
Middle	5847 ± 481	30.9 ± 2.4	10.7 ± 1.7
Mean	4744 ± 1305	32.8 ± 3.8	12.9 ± 3.0
Site 3			
Edge	3282 ± 1519	42.9 ± 3.0	6.6 ± 1.3
Middle	4281 ± 1133	43.0 ± 4.2	6.3 ± 1.1
Mean	3781 ± 1318	43.0 ± 3.6	6.5 ± 1.2

lected with a plastic pipette after 0.5 and 1 h and placed onto a GF/C filter (Advantix) to remove excess water. Subsamples of 100 ml were filtered through a GF/C filter soaked in 10 ml of 90% acetone, then placed in a cool, dark room for extraction for 18 h. Subsequently, chl *a* and phaeopigment concentrations were measured on a Turner Designs 10-AU fluorometer (method adapted from Parsons et al. 1984). Clearance rate standardized to 1 g tissue dry weight animal (l g^{-1} DW h^{-1}) was calculated according to Saurel (2008) (Note: The range of variables that apply to Eq. (5) are temperature 6–19°C, [chl *a*] 2–32 µg l^{-1}):

$$CR = [DR \times 100 / (100 - DF)]/\text{chl } a_{eq} \quad (4)$$

$$DF = -16.90 \times \ln(\text{chl } a_{eq}) - 8.962 \times T_w + 0.3962 \times T_w^2 + 128.70 \quad (5)$$

where DR is the defecation rate (µg chl a_{eq} h^{-1}), chl a_{eq} is the chl *a* equivalent concentration (chl a_{eq} = chl *a* + 1.52 Phaeo, µg l^{-1}) in the surrounding water 2 h prior to the experiment (to take into account the gut residence time) and DF is the digestion factor (%). T_w is the mean seawater temperature during the experiment. Clearance rate estimations were standardized to a 1 g mussel using an allometric factor of 0.67 according to the following equation:

$$Y_s = (W_s/W_e)^{0.67}\ Y_e \quad (6)$$

where Y_s is the standardised parameter, W_s is the standardised weight (1 g), W_e is the weight of the experimental animal and Y_e is the uncorrected parameter (Hawkins et al. 1996).

Data analysis

Paired *t*-tests, 2-sample *t*-tests and ANOVA were used to test for significant differences among datasets, after checking that the data met the assumptions of normality and homogeneity of variance, applying the appropriate transformation ($\log_{10}$ or square root) when necessary. When significant differences were detected, a post-hoc Tukey's multiple comparison test was performed. Statistical analyses were undertaken using Minitab® (v14) and R (www.r-project.org/).

For the analyses of the vertical profile of [chl *a*] above the 2 different treatments (bare or mussel covered substratum), following interpretation of the interaction plots (Fig. 4) a factorial analysis of variance with interaction was applied using the following model:

$$Chl_{ijkl} = \mu + \alpha_i + \beta_j + \gamma_{ij} + (\alpha\beta)_{ij} + (\alpha\gamma)_{ik} + (\beta\gamma)_{jk} + (\alpha\beta\gamma)_{ijk} + \varepsilon_{ijkl} \quad (7)$$

or

$$(Chl)_{ijkl} = \mu + (\text{treatment})_i + (\text{height})_j + (\text{time})_k + (\text{treatment} \times \text{height})_{ij} + (\text{treatment} \times \text{time})_{ik} + (\text{height} \times \text{time})_{jk} + (\text{treatment} \times \text{height} \times \text{time})_{ijk} + \varepsilon_{ijkl} \quad (8)$$

where Chl is the replicate observation of the response variable chl *a* concentration, µ is the overall population mean of the response variable, α, β, γ are the fixed effect associated with the different factor treatments, height (above the bed) and time, and ε_{ijkl} is the error (or residual). An unbalanced design was chosen for the factorial analyses on July 15, 17 and 19 due to some missing samples and an ANOVA model type III SS was applied (Quinn & Keough 2002). The statistical null hypothesis 'there are no 2- or 3-way interactions between the factors (height, time and treatment)' was rejected for the experiments for July 15 and 17, and was only rejected for the interaction of height and time for the experiment on July 19. A further analysis of the simple main effect to test the effect of height for each treatment separately (bare or mussel substratum) was also conducted. The residuals for the linear model were normally distributed (>95% data) and Cook's distance was <0.5.

RESULTS

General description of the system

Hydrodynamics

The flow direction above the mussel bed was multidirectional (note that at low tide, the study area was dried out). The flow turned consecutively in 3 different directions: flow was to the south-east direction when the tide was flooding, then as the tide changed, the direction veered toward the south-west and eventually had a north-westerly direction (Fig. 3). The roving ADCP data revealed that similar types of current regimes occurred at the 3 sites chosen for the experiment. It is important to note that in this system, high water and low water do not coincide with the lowest current velocities.

Seston

The pattern of chl *a* concentration over the mussel bed was correlated with water depth, however this

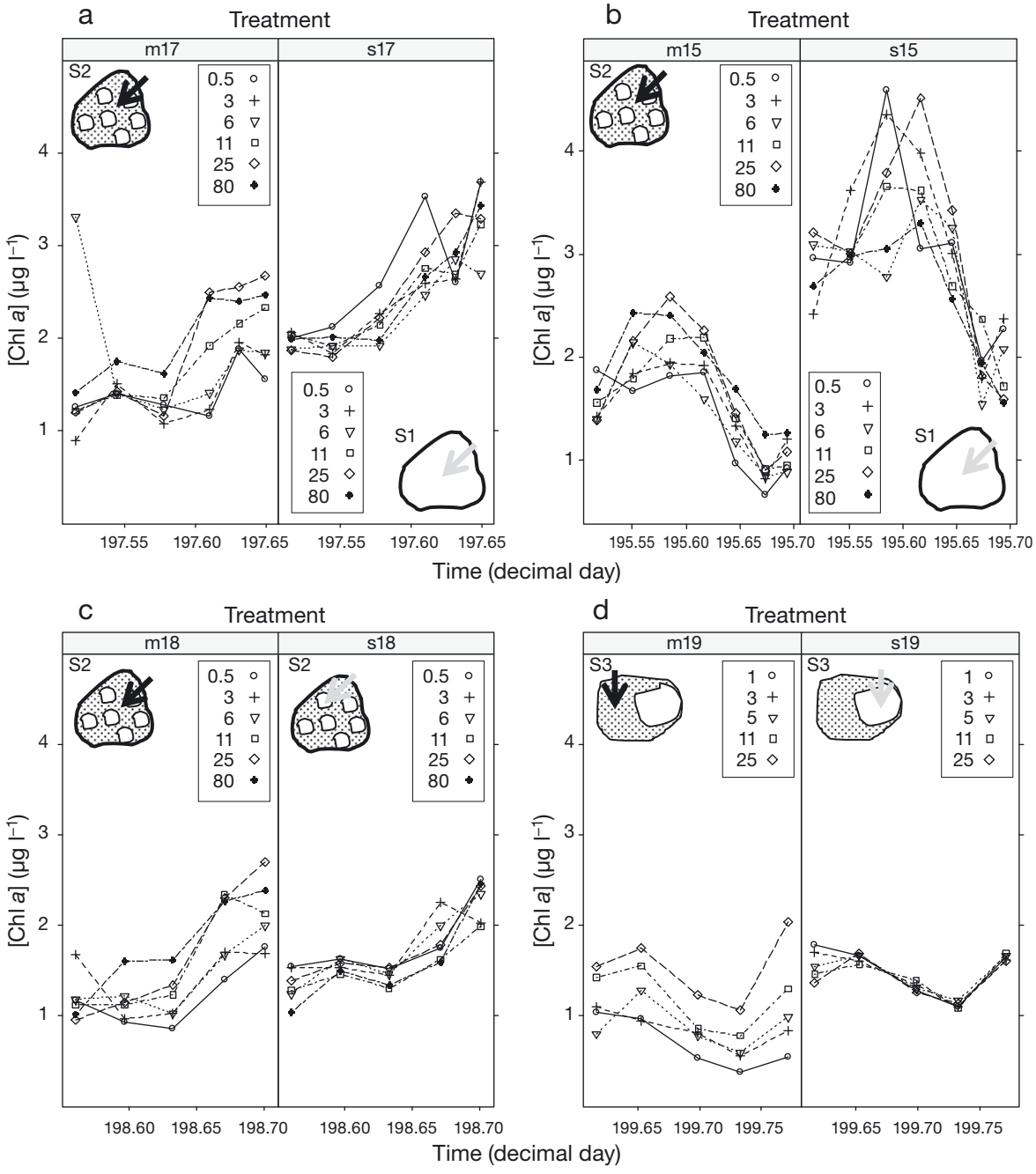

Fig. 4. Mean chl *a* concentration at different depths (0.5–80 cm above the bed) for 2 treatments: with mussel (mdate, left panel) or with bare substratum (sdate, right panel) with repeated samples over tide (Time) for 4 experiments: comparison between Site 1 (S1, bare substratum) and S2 (mussel patch) on (a) July 17 and (b) July 15; and between adjacent mussel and bare substratum patches on (c) S2 on July 18 and (d) S3 on July 19. Arrows as in Fig. 2

was probably related to tidal advection, i.e. chl *a* rich water entering the Menai Strait from Liverpool Bay as a result of the residual flow towards the south west and by the tidal advection of chl *a* depleted water from the Caernarfon Bay end of the Strait during the flow to the north east (Tweddle et al. 2005) (Figs. 5 & 6). The water transported from the intertidal region that had already passed over the mussel beds had depleted chl *a* concentration when it passed back over the experimental mussel bed (Saurel et al. 2007) (Figs. 5 & 6).

Mussels

Overall mussel length was density-dependent although this varied among sites (ANOVA $F_{1,36} = 5.04$;

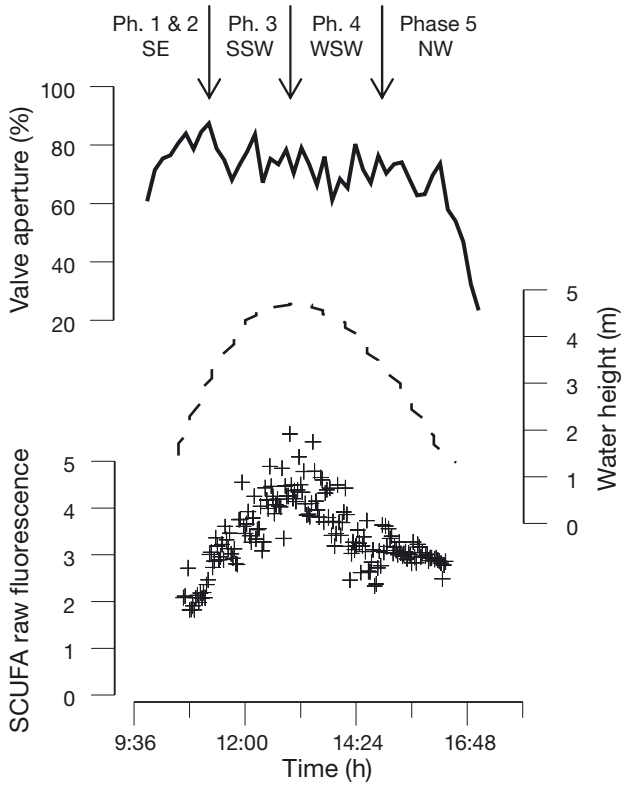

Fig. 5. Mean percentage valve gape aperture (solid line), water height (dashed line) and raw fluorescence from SCUFA (crosses) from July 14 with arbitrarily determined phases of the tide as a function of current direction (see Table 7)

p = 0.031). Shell length was negatively correlated with mussel density in the patch sampled at Site 2 (Pearson Site 2 r = –0.56, p ≤ 0.001) but not at Site 3 (Pearson r = 0.013, p = 0.936) (Table 2). There was no significant difference in density (2-sample *t*-test: t_3 = –0.91, p = 0.428) and shell length between the edge and the middle of the patch at Site 3 (2-sample *t*-test: t_{34} = 0.08, p = 0.936). The mean percentage valve gape aperture showed a similar pattern for each day at Site 2, where mussels were observed filter-feeding with a valve aperture of >60% for 90% of the time during which observations were made (Fig. 5). The general pattern observed was for mussels to open rapidly (40 to 80% valve aperture in <1 h) as soon as the water flooded onto the intertidal bed and the fluorescence increased in the water column. Then, a constant aperture of between 60% to a maximum aperture width of 80% occurred during the remainder of the tide while there was a high level of fluorescence (Fig. 5), until one hour before low tide when fluorescence was reduced (Fig. 5). In the last hour of the ebb, there was a reduction in the valve gape until total closure occurred when the mussels were exposed to the air at low tide.

Comparison of turbulent mass transport and feeding rate

Vertical mixing

The mean vertical diffusivity estimated from the ADCP at 0.05 m above the mussel bed was 2.03 × 10^{-4} ± 1.03 × 10^{-4} m^2 s^{-1} for the first 12.4 h from low tide on the first sampling day (July 15, Site 2) and 2.253 × 10^{-4} ± 8.3 × 10^{-5} m^2 s^{-1} for the first 12.4 h from low tide on the second day (July 17, Site 2). K_z decreased with time from the low tide (Fig. 7)

Feeding rate

The mean clearance rate calculated from the defecation method on mussels from site 2 was high: 2.93 ± 1.56 l ind.$^{-1}$ h^{-1}, or 7.40 ± 3.52 l g^{-1} DW h^{-1} (mean water temperature 17.2°C; 1.0 < [chl *a*] < 3.15 µg l^{-1}). The volume of water filtered by the mussels adjusted to the calculated mussel population on both sites varied from 107 to 211 m^3 m^{-2} d^{-1} (Table 3).

Food depletion

With no mussel filtration (bare substratum), no food depletion occurred close to the bed, while there was food depletion vertically in the water column above mussel patches (Figs. 4 & 8).

On four sampling occasions, the comparison of the vertical profiles above the mussel bed with the vertical profiles above a sandy site or between the mussel patch and an adjacent bare patch showed that there were interactions between the height, time and treatment used on both the mussel covered and bare substratum (see Fig. 4). From the analysis of the main model effects, we concluded that only the mussel substratum had an effect on the chl *a* concentration with height, and that this was only statistically significant for 2 out of the 4 experiments for which significant food depletion was measured at a height of <11 cm above the mussel bed (July 17, $F_{5,109}$ = 4.71, p ≤ 0.001; July 19, $F_{1,94}$ = 17.58, p ≤ 0.001) (Tables 4 & 5, Fig. 4). On July 15 and 18, the pattern was similar, but not statistically significant (July 15, $F_{5,116}$ = 2.08, p = 0.07; July 18, $F_{1,8494}$ = 1.83, p = 0.115). In general [chl *a*] at 80 cm above the bed was greater than [chl *a*] at 0.5 cm above the bed for the mussel treatment, while the reverse was observed for the bare substratum treatment. Nevertheless, the statistical results showed that there was no significant difference in the chl *a* concentration with height above the bare substratum (Tables 4 & 5, Fig. 4).

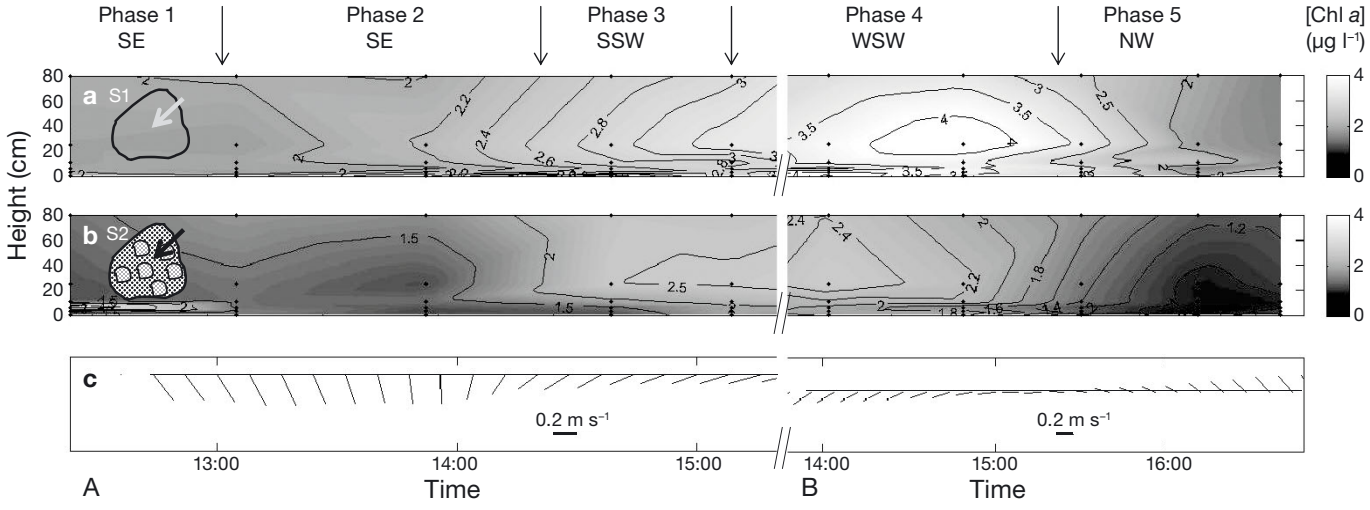

Fig. 6. Vertical profile of chlorophyll *a* concentration (µg l^{-1}) variation with time and height above (a) Site 1, sandy bare substrate and (b) Site 2, mussel bed patch. (c) Depth-averaged current velocity and direction (m s^{-1}) from the ADCP represented by vectors over Site 2 with arbitrary determined phases of the tide as a function of current direction (see Table 7). The origin of the vector is on the horizontal line. Over the whole sampling period, similar data were measured. The data on the left (A) were measured on a rising tide on July 17 while the data on the right (B) were measured on a falling tide on July 15

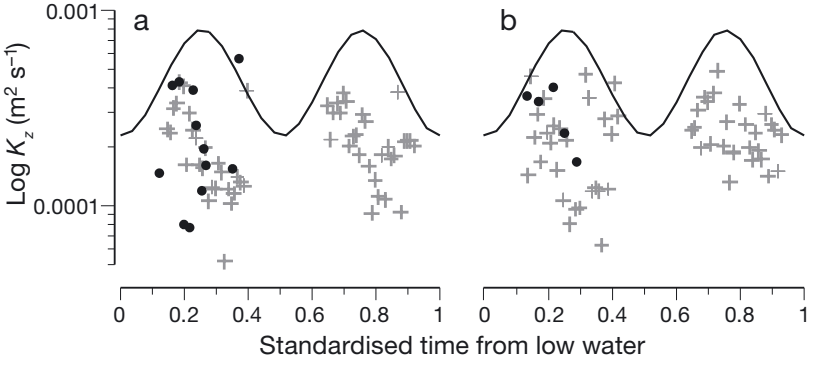

Fig. 7. Diffusion coefficient K_z on logarithmic scale estimated from the ADCP (plus sign) and calculated via the animals (solid circles) with time calculated from low water (1 lunar cycle = 24.84 h) for (a) Site 2 and (b) Site 3. Depth pattern above the bed is represented by a solid black line

Comparison

The results of the K_z estimated from the ADCP were of the same order of magnitude as the K_z calculated from the variation of chl *a* concentration with height (d[chl *a*]/d*z*) and the mean feeding rate of the mussels (Fig. 7). There was considerable variation in the results for measures of both the turbulent transport and feeding rate (see Table 6) that may be attributable to the varying environmental conditions of the tidal cycle (direction of the current, food concentration, velocity).

Bare patch replenishment and re-suspension

A key finding was that food replenishment took place above the bare patch at both Sites 2 and 3. There was a higher concentration of chl *a* at the beginning of the tide (first sampling) at the bottom of the sampled water column above the bare patches than at the top which indicated that re-suspension of the sediment and chl *a* may have occurred (Fig. 4). These results were confirmed from the horizontal profile

Table 3. Estimated volume of water filtered by the mussel populations at Sites 2 and 3 (assuming same individual specific clearance rate [CR] for both sites). Values are ± SD, where applicable. DW: dry weight

	Individual DW (g)	Est. population N	Est. population DW (g)	Mussel cover (%)	CR (l $ind.^{-1}$ h^{-1})	CR (l g^{-1} DW h^{-1})	Volume filtered (m^3 m^{-2} d^{-1}) Mean	Volume filtered (m^3 m^{-2} d^{-1}) if 100% cover
Site 2	0.255 ± 0.083	174.171×10^6	36.576×10^6	63	2.93 ± 1.56	7.40 ± 3.52	211.17	333.6
Site 3	0.268 ± 0.061	70.092×10^6	18.785×10^6	40	2.93 ± 1.56	7.40 ± 3.52	107.15	265.88

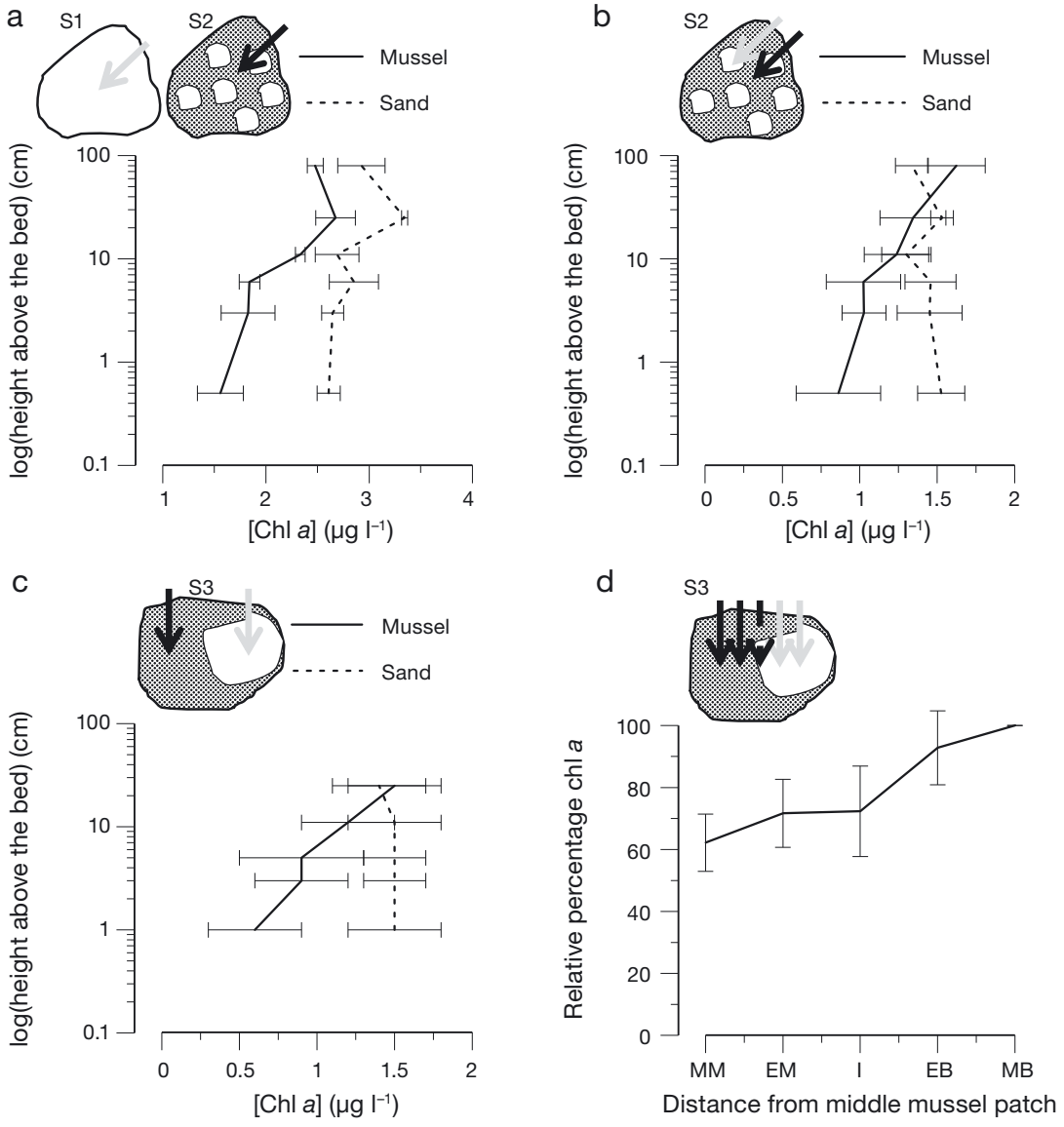

Fig. 8. Example of vertical chl *a* profiles above (a) the sandy Site 1 and the middle of the mussel patch Site 2 (July 17, 2006, 16:34 h), (b) the mussel and adjacent bare patches in Site 2 (July 18, 2006, 16:11 h), (c) the mussel and adjacent bare patches in Site 3 (July 19, 2006, mean of 5 consecutive samplings), (d) horizontal profile between the middle of the mussel patch (MM) and the middle of the adjacent bare patch (MB) for the mean percentage chl *a* concentration, relative to maximum concentration measured in the middle of the bare patch at 5 cm above the bed (July 19, 2006, mean of 5 consecutive samplings). Error bars = standard deviations. EM: edge mussel; I: interface mussel–bare; EB: edge bare patch. Arrows as in Fig. 2

undertaken on July 19 at Site 3 (with samples taken at 5 cm above the bed) between the mussel patch and the adjacent bare patch. This survey showed a lower concentration of chl *a* at the centre of the mussel patch with an increasingly higher concentration toward the middle of the adjacent bare patch (Table 5, Figs. 4d & 8d).

Using the SM, the vertical profiles of chl *a* and phaeopigments concentrations measured over the mussel patch and the bare patch at Site 3 suggested that re-suspension occurred at the beginning of the flood tide (first sampling 14:48 h, GMT i.e. 1.7 h after flooding) when the current velocity was strongest (u = 0.35 m s^{-1}, direction 204°) and at a height of <5 cm above the seabed. A high concentration of phaeopigments occurred at 3 cm above the mussel bed during the first sampling period (ANOVA $F_{4,9}$ = 8.32, $p \leq 0.001$) while no significant difference in phaeopigment concentration was found between the 5 heights measured after the first sampling period

Table 4. ANOVA (type III test for unbalanced design) on July 15, 17 and 19: (a) the full model with the interactions and (b) analysis of the simple main effect to test the effect of height for each treatment (bare or mussel substratum) separately

(a) Full model with interactions					(b) Simple main effect				
Source	df	SS	*F*	p		df	SS	*F*	p
July 17 – No transformation									
Intercept	1	4.71	202.39	≤0.001	Mussel				
Height (H)	5	2.11	18.16	≤0.001	Intercept	1	29.16	130.83	≤0.001
Treatment (Treat)	1	0.67	28.88	≤0.001	Height	5	5.25	4.71	≤0.001
Time	5	0.78	6.67	≤0.001	Residuals	109	2.54		
H × Treat	5	1.75	15.04	≤0.001					
H × Time	25	6.32	10.87	≤0.001	Bare				
Treat × Time	5	3.25	27.94	≤0.001	Intercept	1	87.57	247.66	≤0.001
H × Treat × Time	25	4.88	8.39	≤0.001	Height	5	1.40	0.79	0.56
Error	109	2.54			Residuals	109	2.54		
Total	180	27.02							
July 15 – Square root transformation									
Intercept	1	3.74	672.13	≤0.001	Mussel				
Height	5	0.07	2.36	<0.05	Intercept	1	22.73	520.39	≤0.001
Treatment	1	0.09	15.51	≤0.001	Height	5	0.45	2.08	0.07
Time	6	0.84	25.01	≤0.001	Residuals	116	0.65		
H × Treat	5	0.08	2.80	<0.05					
H × Time	30	0.37	2.20	<0.01	Bare				
Treat × Time	6	0.22	6.47	≤0.001	Intercept	1	42.48	646.80	≤0.001
H × Treat × Time	30	0.58	3.44	≤0.001	Height	5	0.23	0.70	0.628
Error	116	0.65			Residuals	116	0.65		
Total	200	6.61							
July 19 – No transformation									
Intercept	1	2.17	52.64	≤0.001	Mussel				
Height	4	1.07	6.49	<0.01	Intercept	1	6.35	63.094	≤0.001
Treatment	1	0.67	16.18	<0.01	Height	4	7.08	17.581	≤0.001
Time	4	0.89	5.38	≤0.001	Residuals	94	3.87		
H × Treat	4	1.01	6.15	≤0.001					
H × Time	16	1.41	2.14	<0.05	Bare				
Treat × Time	4	0.17	1.02	0.401	Intercept	1	29.30	320.891	≤0.001
H × Treat × Time	16	0.74	1.12	0.350	Height	4	0.12	0.318	0.865
Error	94	3.87			Residuals	94	3.87		
Total	144	11.98							

(ANOVA $F_{4,10} = 1.59$, p = 0.251). During the first sampling period there was a significantly higher concentration of phaeopigments at 1 and 3 cm above the bare patch, in comparison to the rest of the water column (ANOVA $F_{4,10} = 33.7$, p ≤ 0.001).

DISCUSSION

Our study has provided new empirical data on the interaction between the processes that determine carrying capacity for mussel production (seston, hydrodynamic and mussel feeding). The combination of *in situ* measurements of vertical gradients of chl *a*, vertical diffusivity, mussel clearance rate and a simple model (Eq. 2) enabled us to demonstrate that feeding rates closely matched the rates of turbulent transport of [chl *a*] to the mussel bed, and that the food depletion in the BBL was due to mussel filtration. It also showed that the mussel bed patterning, i.e. the presence of bare patches within the mussel bed, facilitated the replenishment of seston and could thereby increase mussel carrying capacity. The dual 'ask the animals — ask the water' approach suggested by Petersen (2004) used in this study gave similar rates of chl *a* transport to the mussel bed and mussel feeding, indicating that the methodologies used are robust and applicable to other systems. Either approach could be used to estimate the feeding rate or to calculate the potential food availability within a system.

Table 5. ANOVA (type II for balanced design) on July 18 for the vertical profile and on July 19 for the horizontal transect: (a) the full model with the interactions and (b) ANOVA of the simple main effect height for each treatment separately for July 18, and Tukey post-hoc analysis for July 19. M stands for mussel substratum, I for interface mussel/bare substratum and S for bare substratum

(a) Full model with interactions

Source	df	SS	*F*	p
July 18 – Square root transformation				
Height (H)	5	0.09	2.20	0.058
Treatment (Treat)	1	0.27	32.14	≤0.001
Time	4	3.79	112.10	≤0.001
H × Treat	5	0.48	11.31	≤0.001
H × Time	20	0.56	3.35	≤0.001
Treat × Time	4	0.23	6.68	≤0.001
H × Treat × Time	20	0.32	1.89	<0.05
Error	120	1.01		
Total	180	6.75		

(b) Simple main effect

	df	SS	*F*	p
Mussel				
Height	5	2.63	1.83	0.115
Residuals	84	24.14		
Bare				
Height	5	1.05	1.18	0.327
Residuals	84	15.08		

Source	df	SS	*F*	p
July 19 – No transformation, horizontal transect				
Treatment	2	0.71	32.53	≤0.001
Time	4	0.97	33.35	≤0.001
H × Treat	5	0.09	1.14	0.351
Error	59	0.64		
Total	73			

Tukey	diff.	p
M vs. I	−0.04	0.446
S vs. I	0.17	≤0.001
S vs. M	0.21	≤0.001

Table 6. Comparisons of diffusion coefficient K_z and CR measured or calculated via ADCP, mussel and seston at Site 2

	Water	Animals
Measured (sampled)	From ADCP $K_z = 2.03 \times 10^{-4} \pm 1.03 \times 10^{-4}$ m^2 s^{-1}	From mussels and seston CR = 2.93 ± 1.56 l ind.$^{-1}$ h^{-1}
Calculated	From K_z ADCP and seston CR = 2.36 ± 1.77 l ind.$^{-1}$ h^{-1}	From mussels and seston $K_z = 2.08 \times 10^{-4} \pm 1.52 \times 10^{-4}$ m^2 s^{-1}

Ecological consequences

Growth in the intertidal mussel bed was limited by the hydrodynamic conditions at Site 2 in the Menai Strait. This conclusion is based on the observed food depletion at the site with concentrations near the mussel bed ~1 µg chl *a* l^{-1}. Further, calculating the food supply to a homogenous mussel bed knowing the measured combination of K_z ($0.1 < K_z < \sim 0.4 \times 10^{-4}$ m^2 s^{-1}) and chl *a* concentration (~1.88 µg chl *a* l^{-1} at $h > 11$ cm and 1.30 µg chl *a* l^{-1} at $h < 6$ cm) would allow for the mussels to reach a clearance rate of 4 l h^{-1} and would support an optimal population density of 800 to 3200 ind. m^{-2}. However, the actual density at Site 2 was 4744 ind. m^{-2}. We conclude that the mussel growers had greatly over-stocked this area. Growth limitations became apparent as the mussels at the Site 2 were from the same cohort with a similar size, were re-laid randomly at the same time but still showing differences in shell length between the edge and the middle of the patch. Similar differences between location in mussel beds have been recorded before and attributed to density-dependence (e.g. Svane & Ompi 1993, Okamura 1986, Fréchette et al. 1992), however in this study it is apparent that the density-dependence is driven by a lack of food, whereas at Site 3 no such growth gradient is seen due to a high availability of food. However, at Site 3 the total mussel coverage (i.e. the percentage occupied by mussel patches) was only 40 % compared to 63 % coverage at Site 2. With less coverage, more gaps between mussel patches are possible; hence, more seston can be replenished in the gap and sustain smaller mussel patches with large mussels at a higher high density. The mussel farmers who utilise this area of seabed have typically attempted to stock the area with as many mussels as possible to counteract the effects of predation, however the present study strongly suggests that such an approach merely leads to poor growth and potential starvation through competition within monocultures of mussels.

The physical and biological processes that occur in the intertidal bed were altered by bed morphology and patterning. In contrast to systems with natural mussel settlement (e.g. the Wadden Sea, van de Koppel et al. 2005; Maine, USA, Snover & Commito 1998), the bed patterning in the Menai Strait evolves during the culture process and is influenced by natural processes (self-organisation/ intraspecific facilitation, van de Koppel et al. 2008; dislodgement/erosion, Bertness & Grosholz 1985, Murray et al. 2002; predation, Okamura 1986) but also by the mussel re-laying process, i.e. flattening of the bed prior to the re-laying, and the pattern of relaying from vessels. Within discrete mussel beds, mussel-covered and mussel-free patches of substratum were similar in size (~5 m wide) compared with those found in other studies (Wadden Sea, ~6 m, van de Koppel et al. 2008; Menai Strait, 2.3–3.1 m, Gascoigne et al. 2005). The shape of the bare patches in the Menai Strait was approximately circular, in comparison to the banded pattern observed in the Wadden Sea (van de Koppel et al. 2005). This could be explained by the manner in which the mussels are relaid by the mussel farmers as well as the influence of tidal currents that transport food from 3 main directions. The bare patches that occurred within the mussel bed allowed seston replenishment due to vertical mixing and also increased the food source derived from the resuspension of microphytobenthos adjacent to the mussels. Re-suspension of microphytobenthos is likely to be an important source of food only at the beginning of the flood tide when current velocity and vertical mixing were highest (Widdows et al. 2009).

BBL and methods limitations

Measuring in or within the BBL *in situ* is challenging, as it is difficult to avoid interference of the instruments with the natural processes and at the same time sample sufficient data to cover natural oceanographic variations. To obtain an acceptable compromise on this issue, we used non-intrusive equipment such as the self-logging ADCP, SCUFA and siphon mimics to avoid interference with the BBL structures. However, variability will still be present in the data due to the inherent fluctuations of turbulence. In contrast to some previous *in situ* studies (e.g. Fréchette & Bourget 1985b) we sampled at a control site without mussels. The vertical profiles at the control site showed neither deposition nor depletion (Table 4), which supported our conclusion that the food depletion in the BBL was due to mussel filtration only. Jones et al. (2009) considered 2 other alternative mechanisms for food depletion in the BBL: (1) the turbulent deposition and (z) near-bed aggregation or near-bed 'fluff layer'. Turbulent deposition of the phytoplankton cells to the sediment can be discarded as a plausible mechanism based on both our results and those of Jones et al. (2009). Besides differences between the study location of Jones et al. (2009) and our study regarding substrate type (clay with high organic content versus sandy-muddy substrate in Menai Strait) and fauna (infaunal clams and polychaetes versus epifaunal mussels in Menai Strait), the main difference is that Jones et al. (2009) did not sample between 0 and 10 cm above the mussel bed. Using the siphon mimic technique we were able to sample 0.5, 3, 6, 11 cm above the bed and we did not find an increase in the local concentration of chl *a* below 10 cm (see Fig. 4). It thus does not seem that a near-bed 'fluff layer' exists at our site and depletion of food can be attributed to mussel filtration.

Our ability to sample very close to the bed may also have affected calculated mass transfer velocity of phytoplankton to the bed (i.e. α, the flux to the bed normalized by near-bed concentration). Using Eq. (8) in Monismith et al. (2010) to compare our results with other recent studies, our calculated α (median Site 2: 98.4 ± 75.1 m d^{-1}; median Site 3: 337.8 ± 92.8 m d^{-1}) was higher than the value found by Monismith et al. (2010) and Jones et al. (2009) (medians 48 ± 20 m d^{-1} and ~50 to 60 m d^{-1}, respectively). We attribute this difference to the high bed shear stress (from 7 × 10^{-3} m s^{-1} to 2.25 × 10^{-2} m s^{-1}) and the fine-scale sampling of seston in the BBL close to the bed ([chl *a*] at 0.5 or 1 cm and [chl *a*] at 25 or 80 cm) in our study.

Feeding rate

When comparing our rates of turbulent transport of chl *a* to the mussel bed or the mass transfer velocity of phytoplankton to the bed calculated as α according to Jones et al. (2009) and Monismith et al. (2010) with feeding rates estimated from the defecation method, the results were in the same range (α from filtration rate ~245–420 m d^{-1}). Mussels fed at high rates (mean CR = 2.9 l $ind.^{-1}$ h^{-1}) and the clearance rates were comparable to that measured in the laboratory under optimal conditions (Møhlenberg & Riisgård 1978, Riisgård & Møhlenberg 1979, Riisgård 2001), demonstrating that the high clearance rate measured in the field is possible as long as environ-

mental conditions such as turbulent mixing prevent re-filtration (O'Riordan et al. 1995). Further, feeding was constant over the entire tidal cycle as is evident from measurements of valve aperture that were >70% open during the entire tidal cycle, which indicated a potentially high CR (Riisgård et al. 2003, 2006, Saurel et al. 2007). Previous studies in the subtidal areas of the Menai Strait demonstrated that at chl *a* concentrations <1 µg l^{-1}, valve aperture was reduced which indicated reduction in filtration rates as also observed in other systems (Saurel et al. 2007).

The total volume filtered by the population (F_{pop}) at Sites 3 and 2 adjusted to the calculated mussel percentage cover was 107.15 m^3 m^{-2} d^{-1} and 211.17 m^3 m^{-2} d^{-1} respectively; these high values are comparable to the higher limit of previous studies in micro- and macro-tidally driven systems such as Kerteminde, Denmark ($38 < F_{pop} < 166$ m^3 m^{-2} d^{-1}; Riisgård et al. 2006) and Oosterchelde, the Netherlands ($31 < F_{pop} < 170$ m^3 m^{-2} d^{-1}; Prins et al. 1996).

Conceptual model

A modified conceptual model of the concentration boundary layer, which develops over a mussel bed with a bare patch in the middle in a unidirectional flow (adapted from Wildish & Kristmanson 1997), is presented in Fig. 9. In this model, water flowing above a mussel bed is depleted of seston in the boundary layer. Once this body of water encounters a bare patch, the lack of a benthic chl *a* sink (i.e. mussels) allows vertical mixing of the near-bed water column, resulting in food replenishment. Therefore, the same body of water is richer in food when it encounters the next mussel patch. Simple calculations can illustrate this model: the bare patches used during the measurements taken with SM were ~5 m wide (almost circular shape), and the food depletion was mainly localised in the water column from the bed to a height of 11 cm. The time necessary to mix this near-bed zone is $t_v = 0.32 \times 0.11^2 / (2.03 \times 10^{-4}) =$ 19 s. The time necessary the water to flow across this bare patch with a mean current speed of 0.25 m s^{-1} (with unidirectional flow) is $t_x = 5/0.25 = 20$ s. Therefore, there is sufficient time for mixing and food replenishment of the <11 cm zone during the transition across a bare patch where no mussel filtration occurs. The implication of this calculation is that the minimum [chl *a*] threshold (<1 µg l^{-1}) at which filtration is reduced or ceases due to valve closure (Riisgård et al. 2003, Saurel et al. 2007) with the same velocity conditions is reached after a water mass has passed across 5 m of mussel bed. Note however, that a threshold of 1 µg chl *a* l^{-1} may not be representative for other bivalve species and in systems with lower or different food concentrations (e.g. Maire et al. 2007, Trottet et al. 2007, Strohmeier et al. 2008).

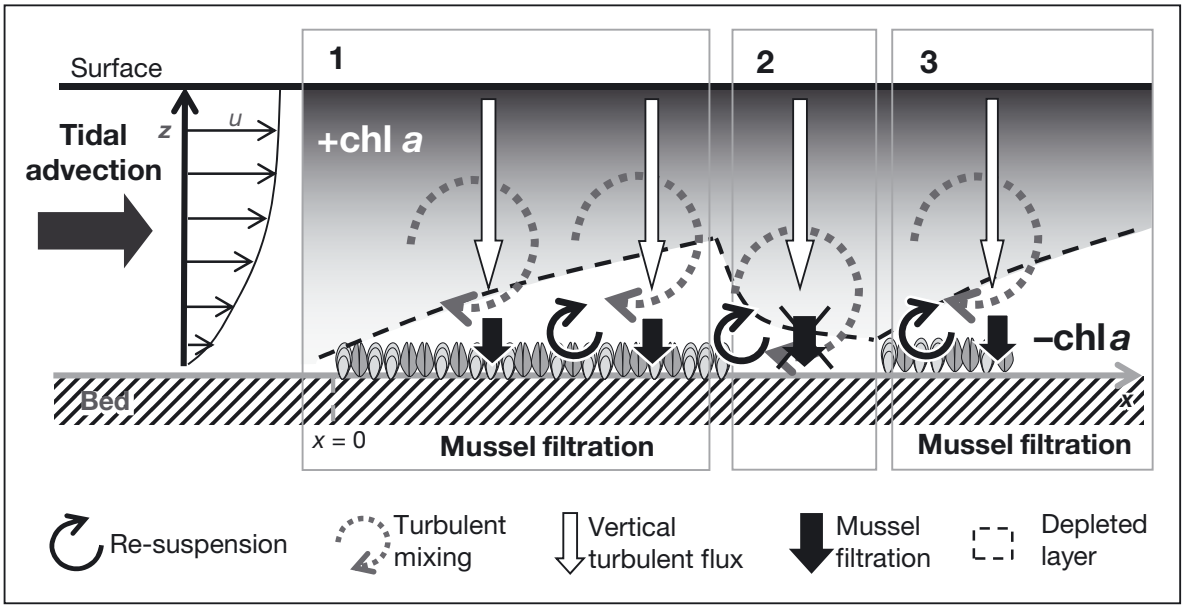

Fig. 9. The concentration boundary layer which develops over a mussel bed with a bare patch in the middle in a unidirectional flow: (1) classical model, (2) situation with bare patch within a mussel bed, (3) classical model after a bare patch. *z*, water depth; *x*, mussel bed length; *u*: velocity; (conceptual model adapted from Wildish & Kristmanson 1997)

Steady-state over a tidal period

The system steady-state was adjusted temporally during the tidal cycle due to the succession of different food sources and hydrodynamic processes (re-suspension, vertical mixing and advection). The tide could be arbitrarily decomposed into 5 phases (Table 7) depending on the processes occurring above the bed. When the water was on the flood (Phase 1) with recycled water from the NE end of the Menai Strait, velocity and vertical mixing were at their highest values, and re-suspension was the main source of food with an increase in phaeopigment concentration near to the bed. In response, the mussels opened their valves rapidly and began filter-feeding. After the initial flood (Phase 2), water velocity decreased and the main supply of food occurred through vertical mixing. Although food concentration was low, the mussels were wide open. In Phase 3, before high tide when the current direction turned and vertical mixing was still the main agent of food supply, the food concentration in the water column started to rise due to the advection of fresh chl *a*-rich new water from Liverpool Bay (Gowen et al. 2000, Tweddle et al. 2005, Saurel et al. 2007, Simpson et al. 2007). At high tide (Phase 4) advection led to the input of a new body of water, vertical diffusion was still strong, and the velocity was low. Eventually the water level declined (Phase 5), the current direction turned, and food depleted water that had already been over the mussel beds was advected above the bed and the strength of the vertical mixing reduced, such that the mussels started to close until the bed was uncovered by water.

SUMMARY

The present study demonstrated that with accurate physical and biological measurements a better understanding of the processes occurring at culture-units (mussel feeding and growth, food concentration, hydrodynamic supply) can be obtained and used for future basin-scale production carrying capacity modelling (Fréchette 2010).

Future management decisions can be based on the simple conceptual model (Fig. 9): knowing the turbulent mixing and chl *a* available to the mussels, density and bare patch size can be modelled for optimising the food availability to the mussel and hence a better production. The optimal size for mussel and patches of bare sediment can therefore be calculated together with the amount of food consumed by the mussel in other systems. Understanding the scale of appropriate patch size to maximize production would improve management decisions about stocking density and would reduce excessive and wasteful initial re-laying of mussel seed. At Site 2 (July 2006), 1 mo after being re-laid the mussel bed appeared to be almost optimally self-organised with (1) the optimal circular bare patch diameter for the turbulent mixing condition of the system (~5 m), and (2) a high density (>4000 ind. m^{-2}), and (3) a high mussel filtration rate (2.9 µg l^{-1}). However, the difference in condition index (CI) between middle and the edge of the mussel patch indicates that growth could have been limited and that a bed with lower density would have been more productive. In contrast, at Site 3 with lower mussel density (<4000 ind. m^{-2}) and percentage cover (40%) than Site 2 (63%), there was no difference in size, density or CI of the mussels at the edge compared to the middle of the patch, indicating that more mussels could have been re-laid on the site.

Table 7. Summary of the hydrodynamics, food concentration and composition, and mussel feeding behaviour in function of the arbitrary determined phases of the tide (tide decomposed into 5 phases). Adv.: advection; HT: high tide; VM: vertical mixing; RW: recycled water; NW: new water

	Phase 1 Flooding	Phase 2 After flood	Phase 3 Before HT	Phase 4 High tide	Phase 5 Ebbing
Hydrodynamics = Main food supplier	Re-suspension VM high	VM high	Adv. VM	Adv. VM	Adv. VM reduces
Velocity	High	Medium	Low	Low	Medium
Current direction	SE	SE	Turn S	WSW	Turn NW
Food (chl *a*) concentration	Low (RW)	Low (RW)	Rising (NW)	High (NW)	Decreasing (RW)
Phaeopigments	High	Reduce	Low constant	Low constant	Low constant
Feeding behaviour	Fast opening	Wide open	Wide open	Wide open	Slow closing

Acknowledgements. We thank K. Mould (Myti Mussel Ltd.) and J. Wilson (DeepDock) for their collaboration and access to their mussel beds. G. Parry Jones and B. Roberts for field work. J. Gascoigne, V. Prieto Salas, A. Queirós, A. Matkins and K. Gower, for assistance in the field; V. Ellis for support in laboratory and J. van de Koppel (NIOO Holland) for providing aerial photography of the site. We thank A. Rodrigues for the conversations on statistics analyses. We thank anonymous reviewers for their constructive comments on a previous version of this manuscript. This research was supported by grants from BBSRC SIS 1554 and BBSRC D18866.

LITERATURE CITED

Beadman HA, Kaiser MJ, Galanidi M, Shucksmith R, Willows RI (2004) Changes in species richness with stocking density of marine bivalves. J Appl Ecol 41:464–475

Bertness M, Grosholz E (1985) Population dynamics of the ribbed mussel, *Geukensia demissa*: the costs and benefits of an aggregated distribution. Oecologia 67:192–204

Bruno JF, Stachowicz JJ, Bertness MD (2003) Inclusion of facilitation into ecological theory. Trends Ecol Evol 18: 119–125

Butman C, Fréchette M, Geyer W, Starczak V (1994) Flume experiments on food supply to the blue mussel *Mytilus edulis* L. as a function of boundary-layer flow. Limnol Oceanogr 39:1755–1768

Cloern JE (1982) Does the benthos control phytoplankton in south San Francisco Bay? Mar Ecol Prog Ser 9:191–202

de Jager M, Weissing FJ, Herman PM, Nolet BA, van de Koppel J (2011) Lévy walks evolve through interaction between movement and environmental complexity. Science 332:1551–1553

Dolmer P (2000) Algal concentration profiles above mussel beds. J Sea Res 43:113–119

FAO (2012) FAO — Fisheries and Aquaculture Information and Statistics Servic. Available at www.fao.org/fishery/statistics (assessed on the 23 Oct 2012)

Fréchette M (2010) Hierarchical structure of bivalve culture systems and optimal stocking density. Aquacult Int 18: 99–114

Fréchette M, Bourget E (1985a) Energy flow between the pelagic and benthic zones: factors controlling particulate organic matter available to an intertidal mussel bed. Can J Fish Aquat Sci 42:1158–1165

Fréchette M, Bourget E (1985b) Food-limited growth of *Mytilus edulis* L. in relation to the benthic boundary layer. Can J Fish Aquat Sci 42:1166–1170

Fréchette M, Butman C, Geyer W (1989) The importance of boundary-layer flows in supplying phytoplankton to the benthic suspension feeder, *Mytilus edulis* L. Limnol Oceanogr 34:19–36

Fréchette M, Aitken AE, Pagé L (1992) Interdependence of food and space limitation of a benthic suspension feeder: consequences for self-thinning. Mar Ecol Prog Ser 83: 55–62

Fréchette M, Lefaivre D, Butman CA (1993) Bivalve feeding and the benthic boundary layer. In: Dame RF (ed) Bivalve filter feeders in estuarine and coastal ecosystem processes. NATO ASI Ser Vol. 33. Springer-Verlag, Berlin, p 325–369

Gascoigne JC, Beadman HA, Saurel C, Kaiser MJ (2005) Density dependence, spatial scale and patterning in sessile biota. Oecologia 145:371–381

Gowen RJ, Mills DK, Trimmer M, Nedwell DB (2000) Production and its fate in two coastal regions of the Irish Sea: the influence of anthropogenic nutrients. Mar Ecol Prog Ser 208:51–64

Hawkins AJS, Smith RFM, Bayne BL, Héral M (1996) Novel observations underlying the fast growth of suspension-feeding shellfish in turbid environments: *Mytilus edulis*. Mar Ecol Prog Ser 131:179–190

Jones NL, Thompson JK, Arrigo KR, Monismith SG (2009) Hydrodynamic control of phytoplankton loss to the benthos in an estuarine environment. Limnol Oceanogr 54: 952–969

Jørgensen CB, Larsen PS, Riisgård H (1990) Effects of temperature on the mussel pump. Mar Ecol Prog Ser 64:89–97

Kotta J, Møhlenberg F (2002) Grazing impact of *Mytilus edulis* L. and *Dreissena polymorpha* (Pallas) in the Gulf of Riga, Baltic Sea estimated from biodeposition rates of algal pigments. Ann Zool Fenn 39:151–160

Kotta J, Orav-Kotta H, Vuorinen I (2005) Field measurements on the variability in biodeposition and grazing pressure of suspension feeding bivalves in the northern Baltic Sea. In: Olenin RDS (ed) The comparative roles of suspension feeders in ecosystems. Kluwer Academic, Dordrecht, p 11–29

Larsen PS, Riisgård HU (1997) Biomixing generated by benthic filter-feeders: a diffusion model for near-bottom phytoplankton depletion. J Sea Res 37:81–90

Lassen J, Kortegård M, Riisgård HU, Friedrichs M, Graf G, Larsen PS (2006) Down-mixing of phytoplankton above filter-feeding mussels — interplay between water flow and biomixing. Mar Ecol Prog Ser 314:77–88

Lewis R (1997) Dispersion in estuaries and coastal waters. John Wiley, Chichester

Maire O, Amouroux JM, Duchêne JC, Grémare A (2007) Relationship between filtration activity and food availability in the Mediterranean mussel *Mytilus galloprovincialis*. Mar Biol 152:1293–1307

Møhlenberg F, Riisgård HU (1978) Efficiency of particle retention in 13 species of suspension feeding bivalves. Ophelia 17:239–246

Monismith SG, Koseff JR, Thompson JK, O'Riordan CA, Nepf HM (1990) A study of model bivalve siphonal currents. Limnol Oceanogr 35:680–696

Monismith SG, Davis KA, Shellenbarger GG, Hench JL and others (2010) Flow effects on benthic grazing on phytoplankton by a Caribbean reef. Limnol Oceanogr 55: 1881–1892

Murray JMH, Meadows A, Meadows PA (2002) Biogeomorphological implications of microscale interactions between sediment geotechnics and marine benthos: a review. Geomorphology 47:15–30

Newell CR, Wildish DJ, MacDonald BA (2001) The effects of velocity and seston concentration on the exhalant siphon area, valve gape and filtration rate of the mussel *Mytilus edulis*. J Exp Mar Biol Ecol 262:91–111

O'Riordan CA, Monismith SG, Koseff JR (1995) The effect of bivalve excurrent jet dynamics on mass transfer in a benthic boundary layer. Limnol Oceanogr 40:330–344

Okamura B (1986) Group living and the effects of spatial position in aggregations of *Mytilus edulis*. Oecologia 69: 341–347

Parsons TR, Maita Y, Lalli CM (1984) A manual of chemical and biological methods for seawater analysis. Pergamon Press, Oxford

Petersen JK (2004) Grazing on pelagic primary producers —

the role of benthic suspension feeders in estuaries. In: Nielsen SL, Banta G, Pedersen MF (eds) Estuarine nutrient cycling: the influence of primary producers. Kluwer Academic, Dordrecht, p 129–152

Petersen JK, Nielsen TG, van Duren L, Maar M (2008) Depletion of plankton in a raft culture of *Mytilus galloprovincialis* in Ría de Vigo, NW Spain. I. Phytoplankton. Aquat Biol 4:113–125

Prins TC, Smaal AC, Pouwer AJ, Danker N (1996) Filtration and resuspension of particulate matter and phytoplankton on an intertidal mussel bed in the Oosterschelde estuary (SW Netherlands). Mar Ecol Prog Ser 142:121–134

Quinn GP, Keough MJ (2002) Experimental design and data analysis for biologists. Cambridge University Press, Cambridge

Riisgård HU (1991) Filtration rate and growth in the blue mussel, *Mytilus edulis* Linneaus 1758: dependence on algal concentration. J Shellfish Res 10:29–35

Riisgård HU (2001) On measurement of filtration rates in bivalves — the stony road to reliable data: review and interpretation. Mar Ecol Prog Ser 211:275–291

Riisgård HU, Møhlenberg F (1979) An improved automatic recording apparatus for determining the filtration rate of *Mytilus edulis* as a function of size and algal concentration. Mar Biol 52:61–67

Riisgård HU, Kittner C, Seerup DF (2003) Regulation of opening state and filtration rate in filter-feeding bivalves (*Cardium edule, Mytilus edulis, Mya arenaria*) in response to low algal concentration. J Exp Mar Biol Ecol 284:105–127

Riisgård HU, Lassen J, Kittner C (2006) Valve-gape response times in mussels (*Mytilus edulis*): effects of laboratory preceding-feeding conditions and *in situ* tidally induced variation in phytoplankton biomass. J Shellfish Res 25:901–911

Rippeth TP, Williams E, Simpson JH (2002) Reynolds stress and turbulent energy production in a tidal channel. J Phys Oceanogr 32:1242–1251

Saurel C (2008) Mussel production carrying capacity: the need for an *in situ* and multidisciplinary approach. PhD thesis, Bangor University

Saurel C, Gascoigne JC, Kaiser MJ (2004) The ecology of seed mussel beds. Literature Review. Report No. FC1015, http://www.seafish.org/media/Publications/Seed_mussel_review.pdf

Saurel C, Gascoigne JC, Palmer MR, Kaiser MJ (2007) *In situ* mussel feeding behavior in relation to multiple environmental factors: regulation through food concentration and tidal conditions. Limnol Oceanogr 52:1919–1929

Seed R, Suchanek TH (1992). Population and community ecology of Mytilus. In: Gosling EM (ed) The mussel *Mytilus*. Elsevier Science Publishers, Amsterdam, p 87–169

Simpson JH, Berx B, Gascoigne J, Saurel C (2007) Tidal advection and diffusion versus mussel filtration in a tidal channel. J Mar Syst 68:556–558

Snover ML, Commito JA (1998) The fractal geometry of *Mytilus edulis* L. spatial distribution in a soft-bottom system. J Exp Mar Biol Ecol 223:53–64

Stacey MT, Monismith SG, Burau JR (1999) Measurements of Reynolds stress profiles in unstratified tidal flow. J Geophys Res 104:10933–10949

Strohmeier T, Duinker A, Strand Ø, Aure J (2008) Temporal and spatial variation in food availability and meat ratio in a longline mussel farm (*Mytilus edulis*). Aquaculture 276:83–90

Svane I, Ompi M (1993) Patch dynamics in beds of the blue mussel *Mytilus edulis* L.: Effects of site, patch size, and position within a patch. Ophelia 37:187–202

Trottet A, Roy S, Tamigneaux E, Lovejoy C (2007) Importance of heterotrophic planktonic communities in a mussel culture environment: the Grande Entrée lagoon, Magdalen Islands (Québec, Canada). Mar Biol 151:377–392

Tweddle JF, Simpson JH, Janzen CD (2005) Physical controls of food supply to benthic filter feeders in the Menai Strait, UK. Mar Ecol Prog Ser 289:79–88

van de Koppel J, Rietkerk M, Dankers N, Herman PMJ (2005) Scale-dependent feedback and regular spatial patterns in young mussel beds. Am Nat 165:E66–E77

van de Koppel J, Gascoigne JC, Theraulaz G, Rietkerk M, Mooij WM, Herman PMJ (2008) Experimental evidence for spatial self-organization and its emergent effects in mussel beds. Science 322:739–742

van Duren L, Herman PMJ, Sandee AJJ, Heip CHR (2006) Effects of mussel filtering activity on boundary layer structure. J Sea Res 55:3–14

Widdows J, Pope ND, Brinsley MD, Gascoigne J, Kaiser MJ (2009) Influence of self-organised structures on near-bed hydrodynamics and sediment dynamics within a mussel (*Mytilus edulis*) bed in the Menai Strait. J Exp Mar Biol Ecol 379:92–100

Wildish D, Kristmanson D (1997) Benthic suspension feeders and flow. Cambridge University Pres, Cambridges.

Williams E, Simpson JH (2004) Uncertainties in estimates of Reynolds stress and TKE production rate using the ADCP variance method. J Atmos Ocean Tech 21:347–357

Editorial responsibility: Jana Davis, Annapolis, Maryland, USA

Submitted: August 3, 2010; Accepted: February 16, 2013
Proofs received from author(s): June 5, 2013